# Net Radiation Estimated from the FY-2D Data over the Source Region of the Yellow River

Rong Liu
Key Laboratory of Land Surface Process and Climate Change in Cold and Arid Regions, Cold and Arid Regions Environmental and Engineering Research Institute, Chinese Academy of Sciences, Lanzhou, Gansu 730000, China,
Email: rliu@lzb.ac.cn

Jun Wen*, Xin Wang, Yue Kang, Yu Zhang
Key Laboratory of Land Surface Process and Climate Change in Cold and Arid Regions, Cold and Arid Regions Environmental and Engineering Research Institute, Chinese Academy of Sciences, Lanzhou, Gansu 730000, China,
Email: jwen@lzb.ac.cn, xinwang@lzb.ac.cn, yuekang@lzb.ac.cn, yuzhang@lzb.ac.cn

***Abstract*— Numerous studies have developed algorithms for estimating the net radiation by satellite remote sensing data obtained under clear sky conditions using polar orbiting meteorological satellite. However, estimating net radiation under cloudy sky conditions using geostationary meteorological satellites with remote sensing sensors remains a significant challenge. In this paper, we developed algorithms to estimate net radiation through the day under all cloud covered conditions using the data from the visible and infrared spin scan radiometer, which is onboard the Chinese geostationary meteorological satellite. The geostationary sensor can be utilized to regularly generate temporally consistent top-of-atmosphere (TOA) and the temperature of brightness blackbody, both at hourly scales because of its frequent temporal sampling (at 1 hour interval). Under the clear sky condition, FengYun-2D (FY-2D) data are used to derive the hourly net radiation. For cloudy case, the transmission coefficient is calculated using TOA reflectance and the attenuation of solar radiation in the atmosphere. Then, amounts of solar radiation under different atmospheric and cloud covered conditions are recorded. The methodology is applied over the source of the Yellow River on September 2009. Compared with ground-based measurements, the root mean square errors of the net radiation estimated under clear and cloudy conditions using the FY-2D data are 27.0W·m-2 and 38.0W·m-2, respectively. The proposed methodology can rely exclusively on remote sensing data in the absence of ancillary ground observations; thus, it can potentially estimate the surface energy budget regionally.**

***Index Terms*—net radiation, cloudy; the source region of the Yellow River, Geostationary Meteorological Satellite**

## I. INTRODUCTION

Net radiation (Rn) is defined as the difference between the incoming and outgoing radiation fluxes, including both shortwave and long radiation, at the Earth's surface. Downwelling short-wave radiation (RS↓) at the surface are resulted from scattering, emission, and absorption within the entire atmospheric column, whereas upwelling short-wave radiation is produced by RS↓ and surface albedo. Downwelling long-wave (RL↓) and upwelling long-wave radiation (RL↑) are characterized by near-surface air temperature, air emissivity, land surface temperature (LST), and surface emissivity [1]. Rn is a key quantity for estimating the surface energy budget and is an important flux that links evaporation, photosynthesis, and heating of soil and air.

Estimating surface net radiation at a high spatial and temporal resolution is challenging. The methodologies for estimating surface Rn or its components (RL↓, RL↑, and RS↓) from satellite data can be classified into two broad categories based on the data used: 1) near-surface data (e.g., land surface temperature, surface albedo, and land surface emissivity); 2) TOA radiation. Several empirical parameterizations have been developed to estimate Rn from near surface data [2-4]. Land surface temperature is commonly obtained directly from remote sensing observation [5] ; land surface albedo and land surface emissivity currents are estimated by radiative transfer models, ancillary ground measurements, and assumptions about certain parameters [6-7]. Downwelling long-wave, one of the main components of Rn, is more difficult to estimate directly from the radiant energy measured using satellite instrument because it is largely decoupled from the radiation measured at the TOA, and mainly comes from the near-surface layers of atmosphere. Studies using TOA radiance involve developing a statistical regression model that incorporates dependence on solar zenith angle and satellite viewing angles [8-9].

Satellites can be either polar orbiting, seeing the same swath of the Earth every 12 hours, or geostationary, hovering over the same spot on Earth by orbiting over the equator while moving at the speed of the Earth's rotation. Various remote sensing platforms are the basis for polar orbiting meteorological satellites, which includes geostationary operational environmental satellites, Advanced Very High Resolution Radiometer (AVHRR), and the MODerate resolution Imaging Spectroradiometer (MODIS). They have been used to estimate components of the surface energy budget [10-13]. Polar orbiting meteorological satellites provide data pertaining to land and atmospheric states with a high-spatial, but low-temporal resolution, compared to ground-based measurements. The geostationary sensor can be utilized

© 2013 ACADEMY PUBLISHER
doi:10.4304/jsw.8.10.2482-2488

to regularly generate temporally consistent fluxes both at hourly and daily time scales because of its frequent temporal sampling (at 60 min or 30 min intervals) [14]. FY-2D is the present on-orbit Chinese geostationary meteorological satellite launched on 8 Dec, 2006 and located at 86.5°E. The major payload is a five-channel Visible Infrared Spin Scan Radiometer (VISSR). This radiometer consists of one broad visible band (VIS; 0.55 μm to 0.90 μm) with 1.25 km spatial resolution, one water vapor band (WV; 6.30 μm to 7.60 μm), and three thermal infrared (IR; 3.50 μm to 4.00 μm, 10.30 μm to 11.30 μm, and 11.50 μm to 12.50 μm) bands, each with a spatial resolution of 5 km [15].

The source region of the Yellow River, located in the middle east of the Tibetan Plateau, significantly affects the climate and ecosystem evolution over the East Asian continent. In the past 30 years, the source of the Yellow River has directly lost 17% of its glaciers and 2.39 billion cubic meters of water. The rate of melting of the ice is 10 times faster than it was in the previous 300 years [16]. Rn is important for the development of the planetary boundary layer, and its quantification over the source of the Yellow River is crucial for studying land–atmosphere interactions. The energy fluxes have been successfully estimated from MODIS data over the Tibetan Plateau [17]. However, few studies have estimated the Rn over the source of the Yellow River using FY-2D geostationary meteorological satellite.

The objective of this study is to improve the understanding of Rn in the source of the Yellow River, especially under cloudy conditions. Thus, we present a method that provides simplified satellite-based Rn estimation using geostationary satellite imagery over large areas. The proposed methodology is intended to avoid numerous surface meteorological observations that are not readily available over large areas. All the data are collected during an experimental campaign in September 2009. Section II presents the framework for estimating Rn under all cloud cover conditions by separately treating clear and cloudy pixels within the FY-2D overpass. Section III describes the study site and the data used, including ground measurements and the FY-2D data products. The instantaneous Rn results using the FY-2D products for all cloud covered conditions are presented and validated in Section IV, also including final results analyzed and discussed.

## II. METHODOLOGY

The net radiation is given by the following equation:

$$R_n = (1-\alpha)Q + L\downarrow - L\uparrow \quad (1)$$

Where α is the surface albedo, which can be determined using satellite remote sensing data; Q is the solar global radiation (W·m-2); L↓ and L↑ are the downward and upward long-wave radiation (W·m-2) respectively.

The downward and upward short-wave and long-wave radiation are calculated with clear sky conditions. On the other hand, only the downward and upward short-wave is calculated with cloudy sky conditions because the values of the downward and upward long-wave are similar [18].

### A. Clear Sky Conditions

For the clear skies, (1) is expressed in terms of downward and upward radiation as:

$$R_n = (1-\alpha)\cdot Q + \varepsilon \cdot R_{lwd} - \varepsilon \cdot \sigma \cdot T_s^4 \quad (2)$$

Where Rlwd is the downward long-wave radiation, ε is the emissivity of the surface, σ is the Stefan–Boltzmann constant (5.669×10−8 W·m-2 k-4), and Ts is the surface radiative temperature. α, ε, and Ts can be derived using remote sensing data from the visible to the thermal infrared spectral range.

The simplest form to calculate the downward solar radiation Q can be estimated with the method founded by Bastiaanssen and Menenti [19]. ε is the land surface effective emissivity, which can be expressed as follows [20]:

$$\varepsilon = 1.0094 + 0.047\ln(NDVI) \quad (3)$$

The downward long-wave radiation cannot be measured directly. It can be calculated as

$$R_{lwd} = \varepsilon_a \cdot \sigma \cdot T_a^4 \quad (4)$$

Where Ta is the air temperature at the reference height, and the emissivity of the atmosphere can be estimated by Campbell and Norman [21] as:

$$\varepsilon_a = 9.2\times10^{-6}\cdot(T_a + 273.13)^2 \quad (5)$$

In summary, the steps for calculating the net radiation under clear sky conditions are: first, the downward short-wave radiation are determined by combining the estimated solar radiation and albedo data using polar orbiting meteorological satellite (FY-3A). Second, the atmospheric downward long-wave radiation is calculated by using the emissivity of the atmosphere, the Stefan–Boltzmann constant, air temperature, and surface emissivity. Finally, the land surface temperature, surface emissivity, and the Stefan–Boltzmann constant are used to estimate the upward long-wave radiation.

### B. Cloudy Sky Conditions

An acceptable clear sky remote sensing image is defined as one wherein 75% of the area is cloud free; thus it is a satisfactory candidate for applying clear sky Rn estimation methodology over the cloud-free portion of the overpass [22]. Only 7% of the NOAA/AVHRR data is available in day and night under acceptable clear sky conditions. Thus, for a large share of remotely sensed data, the Rn cannot be computed using existing methodologies because they are only suitable for clear conditions.

In optics and spectroscopy, transmittance τ is the fraction of the incident radiation at a specified wavelength that passes through a sample. Its formula is as follows:

$$\tau = \frac{Q_S}{Q_0} = \mathrm{e}^{-kx} \quad (6)$$

Where $Q_s$ is the solar radiation received by the land surface, $Q_0$ is the total solar radiation before passing through the atmosphere boundary, and kx is the optical depth.

© 2013 ACADEMY PUBLISHER

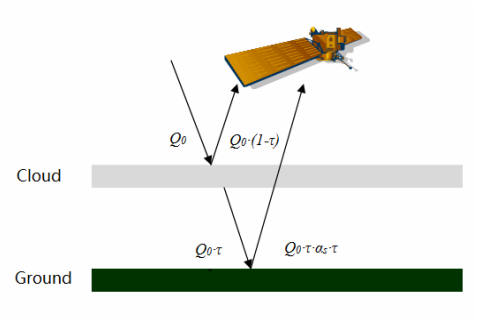


Figure 1. The scheme of energy transmission measured by a sensor.

Fig. 1 shows the scheme of energy measured with a satellite radiometer. According to this scheme, the energy measured by the satellite radiometer is partitioned as follows:

$$\alpha_{TOA}Q_0 = Q_0 \cdot \tau \cdot \alpha_s \cdot \tau + (1-\tau)Q_0 \quad (7)$$

Where, $\alpha_{TOA}$ is the TOA reflectance; $Q_0 \cdot \alpha_{TOA}$ is the energy by received the satellite sensor; $\alpha_s$ is the land surface albedo, $Q_0 \tau \alpha_s \tau$ represents the energy that passes through the atmosphere, reflected by the target, and directly transmitted to the sensor; and $(1-\tau)Q_0$ represents the energy directly reflected back to the sensor at the top of the atmosphere. According to the (7), transmission $\tau$ is given by:

$$\tau = \frac{1-\sqrt{1-4\alpha_s \cdot (1-\alpha_{TOA})}}{2\alpha_s} \quad (8)$$

Where, $\alpha_{TOA}$ and $\alpha_s$ can be obtained from the FY-2D remote sensing data.

Therefore, the solar radiation that reaches the Earth's surface can be obtained by the following expression:

$$Q_S = (1-\alpha).Q_0.\tau \quad (9)$$

The transmission $\tau$ in this equation is not only the transmission that affects the solar radiation but it also incorporates the interaction between absorption and scattering effects.

In summary, the steps to calculate net radiation under cloudy conditions are: the function of transmission and TOA is obtained using the relationship between solar radiation and that received by the satellite sensor. The transmission under any cloud cover and thickness is calculated by the same relationship. Areas with TOA>0.3 and TBB<273 are the areas covered by clouds. The net radiation is calculated using the transmission equation under any cloud cover condition.

## III. CASE STUDY

### A. Area of Study

The region drained by the Yellow River is situated in the eastern part of the Qinghai–Tibet Plateau (31.5°–36.5 N, 95.5°–103.5 E), which has an average altitude of approximately 3000 m and a typical continental monsoon climate.

Fig. 2 shows the land use classification of the study area. The Bayan Har Mountain is on the northwest, and bushes and grass mixed areas surround the Yellow River. It has complex geomorphic features consisting of diverse landscapes, including mixed forest, shrub land, grassland, sparsely pastures, and water bodies. Among these lakes, Lake Gyaring and Lake Ngoring are the biggest.

The experimental site experiences clammy plateau weather. The mean annual temperature is 274.3 K, with a mean minimum of 264.5 K and a mean maximum of 284.5 K. The annual frost-free period is 19 days, whereas and the annual precipitation is 560 mm. The vegetation in the area is typical alpine meadow dominated by graminaceous species, with a canopy height of less than 0.15 m. The main types of soil are alpine meadow soil and swamp soil [23-24].

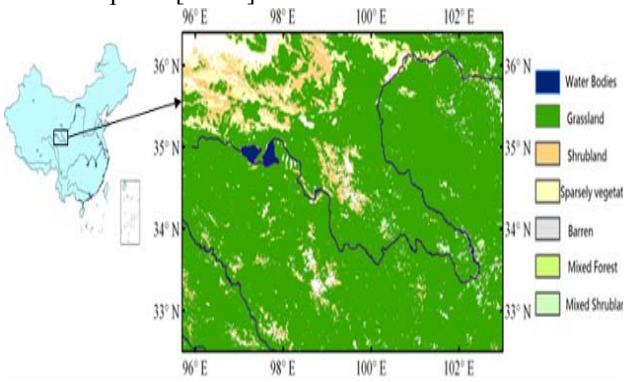


Figure 2. The location of the Yellow River source area and the land use information of the study area

### B. Meteorological Data

The Maqu Climate and Environment Comprehensive Observation Station (33 53′22.7″N, 102 08′27.5″E; elevation, 3443m), located in the Maqu Grassland of the Gannan Tibetan autonomous prefectures in Gansu Province, is in the eastern rimland on the Tibetan Plateau. Among the various Tibet Plateau landscapes, the Gannan Tibetan, wherein the field experimentsare conducted, it is characterized by large flat grass, which has a length from 40 km to 120 km.

The experiment was conducted in September 2009 at the Maqu site. A boundary layer meteorological tower at the station was deployed in 5 levels (1m, 2m, 4m, 8m, and 16m) to measure wind speed and direction, air temperature, and humidity. A solar radiation quantum sensor was mounted at a height of 3.0 m. The eddy covariance instrumentation was oriented to the north, which was the predominant wind direction during the summer season. All the EC system measurement data were routinely checked for quality assurance; various filtering techniques were applied in data pre-processing. The net radiation fluxes were derived from observations by the CRN-1 radiometer systems installed at the site. The soil heat flux was measured using heat transducers (HFT01) at 2.5 cm and 10 cm depths. The flux data were then examined at 10-day intervals, and extreme values and values greater than ±3 standard deviations were removed. For the missing values, the daytime gaps were filled via linear interpolation between the nearest temporal measurements. In addition, an automatic weather station was installed. The measurements included

© 2013 ACADEMY PUBLISHER

the wind velocity and direction at a height of 2.0 m, as well as the temperature and humidity at 1.5 m height during the experimental period.

### C. Satellite Data

Many advances in instrument design and processing algorithms for earth observation have been achieved in the last decade. The geostationary sensor can be utilized to regularly generate temporally consistent energy fluxes hourly and daily because of its frequent temporal sampling (at 30 minute intervals).

The present on-orbit geostationary satellite FY-2D, located at 86.5° E, was chosen for this study. The FY-2D is a spin-stabilized satellite launched on 8th Dec 2006. The major payload for each satellite was a five-channel VISSR. The satellite raw data were handled in a pre-processing system. After quality control, image navigation/registration, calibration, and remapping, the satellite raw data were remapped into normalized image projection. All the information for meteorological product derivation, such as observation time, calibration table, solar zenith angle, satellite view zenith angle, relative azimuth angle, ocean mask, and so on, were attached in a dataset called normalized geostationary dataset(NOM). The NOM dataset was the basis of the FY2 ground system. The 1.25 km visible dataset provides 5km images for all FY2 channels.

FengYun-3A (FY-3A), launched on 27th May 2008, is the second Chinese generation polar-orbiting meteorological satellite. Its missions include monitoring global disasters and environment changes. FY-3A has more powerful spatial resolution than FY-2D because it has sounding capabilities and natural color imagery, with a higher spatial resolution of 250 m. Therefore, the FY-3A data was used to estimate the NDVI, ε, and $\alpha_s$ in our study.

A detailed description of the FY-2D and FY-3A data products is presented as FY-2 satellite products and data format [25] and Yang et al. , 2009 [26]. Additionally, in the present study, we utilized the FY-2D TBB product to determine the land surface temperature [27].

## IV. Results and Validation

The steps for net radiation estimate are: firstly, the NDVI was used to retrieve emissivity from FY-3A data. Secondly, the land surface albedo was estimated using FY-2D data, and land surface temperature was estimated from FY-2D level 2 TBB and emissivity data. Thirdly, the estimated surface albedo and temperature were used to partition componential values of solar radiation that the land surface received under clean and cloudy conditions by (8) and (9). Finally, with the aid of meteorological variables, net radiation was estimated during the day over the source region of the Yellow River.

### A. Land Surface Emissivity

NDVI was calculated using two infrared bands (0.58μm to 0.68μm and 0.84μm to 0.89 μm), and land surface emissivity was obtained by NDVI and Van's method (Van, 1993). Fig. 3 shows the estimated NDVI and emissivity on 7th September 2009 over the source region of the Yellow River by FY-3A and FY-2D data, respectively. The estimated NDVI decreases from north to south, which corresponds to the land use map. The regions of higher value are concentrated on the Maqu area, and its values reached more than 0.50. However, the values were less than 0.10 in the Northeast regions. The

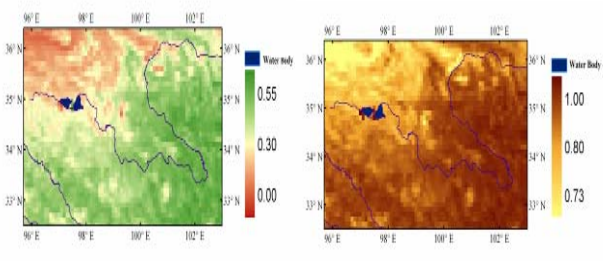


Figure 3. Maps of NDVI and emissivity over the source region of the Yellow River derived from FY-3A and FY-2D on 7th September, 2009

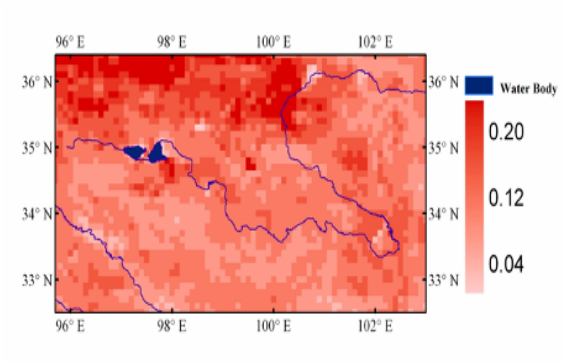


Figure 4. land surface albedo over the source region of the Yellow River from FY-2D on 7th September, 2009

emissivity values were higher in the vegetation area in the southeast and lower in the saline area in the northwest.

### B. Land Surface Albedo

Fig. 4 shows the estimated albedo over the source region of the Yellow River from FY-2D on 7 September 2009. The estimated albedo decreases from north to south, which corresponds to the land use map. The regions of higher value are concentrated at the northwest area because of its saline landscape, and its values could reach more than 0.20. On the other hand, the values were less than 0.10 in the southeast regions, where Maqu station was located.

### C. Land Surface Temperature

Land surface temperature is one of the key parameters in the physics of land surface processes, combining surface-atmosphere interactions and the energy fluxes between the atmosphere and the ground [28]. One month of FY-2D level 2 brightness temperature data from September 1 to 30, 2009, which were obtained from the FENGYUN Satellite Center Data Center.

© 2013 ACADEMY PUBLISHER

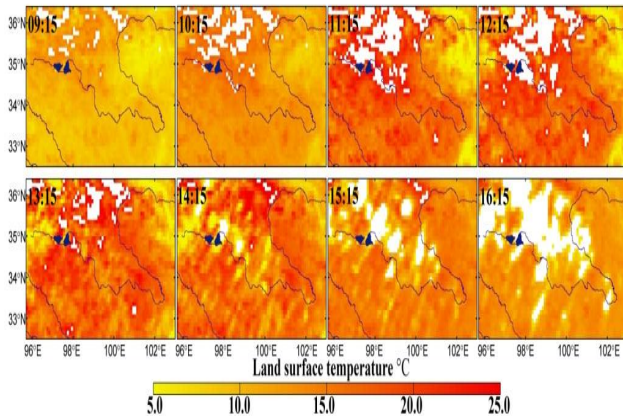


Figure 5. Maps of land surface temperature at different times over the source region of the Yellow River on 7th September, 2009

The product is the 5 km × 5 km grid data re-sampled from FY-2D MWRI. Figure 5 shows the land surface temperature at different times on 7 September 2009, according to brightness temperature data and Planck's law. White parts represent the cloud-covered areas, where temperature is lower than 273 K and albedo is higher than 0.3. The land surface temperatures can vary throughout the day and can range from 5.0 °C to 25.0 °C. Each image from the northwest area exhibits high temperature mainly due to saline and bare soil land. Some of the low temperature zones are also seen near the Yellow River mainly due to wetland use.

### *D. Instantaneous Net Radiation*

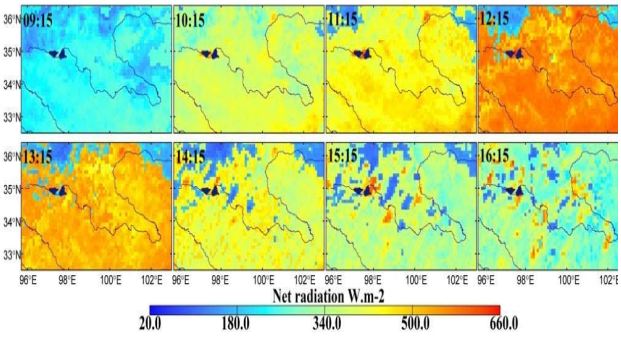


Figure 6. Maps of net radiation at different times estimated by FY-2D over the source region of the Yellow River on 7th September, 2009

Fig. 6 shows the maps of net radiation at different times on 7th September 2009. The results show that the hourly average variation of net radiation is related to land surface temperature, and the dispersion of hourly net radiation fluctuation is low during 9:15 and 16:15, which are the times for sunrise and sunset, respectively. In the Maqu area, as sun elevation angle changes, the value can reach 350.0 W·m-2 at 10:15 and 650W·m-2 at approximately 12:15 (midday). The spatial distribution of net radiation is quite uniform over the whole source region of the Yellow River. The values for cloudy covered areas have distinguishable differences and are generally between 30.0 W·m-2 to 80.0 W·m-2 over the northern lakes basin area from 09:00 to 15:00.

### *E. Validation*

To validate the net radiations of the different times during the day, we need to compare them with ground-based observations from a regional perspective. Ground measurements can provide accurate information and are critical to quantitatively assess remote sensing interactions with land surface properties. However, due to the complexity of natural surfaces, it is more critical for coarse resolution geostationary meteorological satellite measurements at 5km especially.

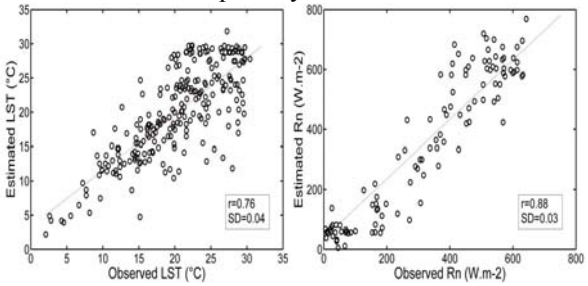


Figure 7. Land surface temperature and net radiation scatters between FY-2D estimates and ground measured.

Fig. 7 shows the inter-compassion of FY-2D estimates and ground-measured surface temperature and net radiation. The remote sensing estimated actual land surface temperature and net radiation show a consistent relationship with simultaneous values of ground measurement. We can also conclude that the error is smaller through this method. The minimum and maximum relative errors are 3.0% and 43.9% for land surface temperature. Without considering the impact of mixed pixel, emissivity, and blackbody, brightness temperature data were used to estimate surface temperature in this paper, which can cause inevitable errors.

The minimum and maximum relative errors were 4.0% and 44.0% for net radiation, whereas the correlation coefficient was 0.88. The low values estimated using our method for grassland were concentrated at sunrise or sunset at which the measured values were less than zero, but the estimates were more than zero. Dew may cause positive bias in surface albedo measurement from moisture condensation because temperature declines in swamp. The albedo, which follows an upward trend from sunrise to mid-day and follows a downward trend after mid-day, appeared to have an asymmetric distribution with the change in sun elevation angle. These comparisons imply that the net radiation assessed using the FY-2D data is in accordance with the field observations.

## ACKNOWLEDGMENT

This work was supported by the West Light Foundation of the Chinese Academy of Sciences (No.No.29Y329941), the National Science Foundation of China (Grant No.41175027), Special Fund for Meteorological Scientific Research in Public Interest (GYHY201106028), the CEOP-AEGIS project funded by the European Commission through the FP7 program and

© 2013 ACADEMY PUBLISHER

open fund from State Key Laboratory of Cryospheric Sciences, Cold and Arid Regions Environment and Engineering Research Institute, Chinese Academy Sciences (SKLCS 2012-10).

## REFERENCES

[1] B. Gautam, R.L. Bras, "Estimation of net radiation from the MODIS data under all sky conditions: Southern Great Plains case study", Remote Sensing of Environment, Elsevier, vol. 114, no. 7, pp.1522-1534, 2010. doi: 10.1016/j.rse.2010.02.007

[2] W. Brutsaert, "On a derivable formula for long-wave radiation from clear skies", Water Resources Research, American Geophysical Union, vol. 11, pp.742−744, 1975. doi: 10.1029/WR011i005p00742

[3] R.T. Pinker, R. Frouin, Z. Li, " A Review of Satellite Methods to Derive Surface Shortwave Irradiance", Remote Sensing of Environment, Elsevier, vol. 51, no. 1, pp.108-124, 1995. doi: 10.1016/0034-4257(94)00069-Y

[4] G. Bisht, V. Venturini, S. Islam, L. Jiang, "Estimation of the Net Radiation Using Modis (Moderate Resolution Imaging Spectroradiometer) Data for Clear Sky Days", Remote Sensing of Environment, Elsevier, vol. 97, p.52-67, 2005. doi: 10.1016/j.rse.2005.03.014

[5] F. Becker, Z.L. Li, "Towards a Local Split Window Method over Land Surfaces. International Journal of Remote Sensing", Taylor & Francis, vol. 11, pp.369-93, 1990. doi: 10.1080/01431169008955028

[6] E. Hurtado, J.A. Sobrino, "Daily Net Radiation Estimated from Air Temperature and NOAA-AVHRR Data: A Case Study for the Iberian Peninsula", International Journal of Remote Sensing, Taylor & Francis, vol. 22, p p.1521-1533, 2001. doi: 10.1080/01431160121189

[7] L. Jiang, S. Islam, "Estimation of Surface Evaporation Map over Southern Great Plains Using Remote Sensing Data", Water Resources Research, American Geophysical Union, vol. 37, no. 2, pp.329-340, 2001. doi: 10.1080/01431160210154821

[8] Z. Li, H.G. Leighton, K. Masuda., T. Takashima, "Estimation of SW Flux Absorbed at the Surface from Toa Reflected Flux", Journal of climate, American Meterological Society, vol. 6, no. 2, pp.317-317, 1993. doi: 10.1175/1520-0442(1993)006<0317

[9] W. Wang, S. Liang, "Estimation of High-Spatial Resolution Clear-Sky Long-wave Downward and Net Radiation over Land Surfaces from Modis Data", Remote Sensing of Environment, Elsevier, vol. 113, no. 4, pp.745-754, 2009. doi: 10.1016/j.rse.2008.12.004

[10] J. Andersen, I. Sandholt, K.H. Jensen, J.C. Refsgaard, Gupta H., "Perspectives in using a remotely sensed dryness index in distributed hydrological models at the river-basin scale", Hydrological Processes, Wiley, vol.16, no. 15, pp.2973–2987, 2002. doi: 10.1002/hyp.1080

[11] B.J. Choudhury, T.J. Dorman, A.Y. Hsu, "Modeled and observed relations between the AVHRR split window temperature difference and atmospheric precipitable water over land surfaces", Remote Sensing of Environment, Elsevier, vol. 51, no. 2, pp.281–290, 1995. doi: 10.1016/0034-4257(94)00087-4

[12] H.A. Cleugh, R. Leuning, Q.Z. Mu, S.W. Running, "Regional evaporation estimates from flux tower and MODIS satellite data", Remote Sensing of Environment, Elsevier, vol. 106, no. 3, pp.285–304, 2007. doi: 10.1016/j.rse.2006.07.007

[13] Z. Su, H. Pelgrum, M. Menenti, "Aggregation effects of surface heterogeneity in land surface processes", Hydrology and Earth System Sciences, Copernicus Group, vol. 3, no. 4, pp.549–563, 1999. doi:10.5194/hess-3-549-1999

[14] M.C. Anderson, W.P Kustas., J.M. Norman, "Upscaling Flux Observations from Local to Continental Scales Using Thermal Remote Sensing", Agronomy Journal, American Society of Agronomy, vol. 99, pp.240-254, 2007. doi: 10.2134/agronj2005.0096S

[15] Y.Q. Shu, S. Stisen, K.H. Jensen, I. Sandholt, "Estimation of regional evapotranspiration over the North China Plain using geostationary satellite data", International Journal of Applied Earth Observation and Geoinformation, Elsevier, vol.13, no.2, pp.192-206, 2011.doi: 10.1016/j.jag.2010.11.002

[16] H. Wang, N.H. Bi, Y.S.K. Saito, Y. Wang, X.X. Sun, J. Zhang, Z.S. Yang, "Recent changes in sediment delivery by the Huanghe (YellowRiver) to the sea: Causes and environmental implications in its estuary", Journal of hydrology, Elsevier, vol. 391, no. 3-4, pp.302-313, 2010. doi: 10.1016/j.jhydrol.2010.07.030

[17] Y. Ma, L. Zhong, B. Wang., W. Ma, X. Chen, M. Li, "Determination of land surface heat fluxes over heterogeneous landscape of the Tibetan Plateau by using the MODIS and in-situ data", Atmospheric Chemistry and Physics, John Wiley &amp, vol. 11, no. 20, pp.10461–10469, 2011. doi: 10.5194/acp-11-10461-2011

[18] W. Xiao, G.N. Flerchinger, Q. Yu, Y.F. Zheng, "Evaluation of the SHAW model in simulating the components of net all-wave radiation", American Society of Agricultural and Biological Engineers, Maney, vol. 49, no. 5, pp.1351−1360, 2006. doi: 10.2134/agronj2005.0126

[19] W.G.M. Bastiaanssen, M. Menenti, R.A. Feddes, A.A.M. Holtslag, "A remote sensing surface energy balance algorithm for land (SEBAL)", Journal of Hydrology, Elsevier, vol. 212, pp.198–212, 1998. doi: 10.1016/S0022-1694(98)00253-4

[20] A.A. Van De Griend, M. Owe, "On the relationship between thermal emissivity and the normalized difference vegetation index for natural surfaces", International Journal of Remote Sensing, Taylor & Francis, vol. 14, no. 6, pp.1119-1131, 1993. doi: 10.1080/01431169308904400

[21] G. S. Campbell, J. M.Norman, "An Introduction to Environmental Biophysics (2nd ed.)", Springer-Verlag, pp.286, 1998.

[22] G. Bisht, V. Venturini, S.Islam, L. Jiang, "Estimation of the Net Radiation Using Modis (Moderate Resolution Imaging Spectroradiometer) Data for Clear Sky Days", Remote Sensing of Environment, Elsevier, vol. 97, no, pp.52-67, 2005. doi: 10.1016/j.rse.2005.03.014

[23] Y.C. Lan, G.H Zhao., Y,N, Zhang, J. Wen, J.Q. Liu, X.L. Hu, "Response of runoff in the source region of the Yellow River to climate warming", Quaternary International, Elsevier, vol. 226, no. 1-2, pp.60-65, 2010. doi: 10.1016/j.quaint.2010.03.006

[24] X.S. Yi, G.S. Li, Y.Y. Yin, "The impacts of grassland vegetation degradation on soil hydrological and ecological effects in the source region of the Yellow River—A case study in Junmuchang region of Maqin country", Procedia Environmental Sciences, Elsevier, vol. 13, ,pp.967-981, 2012. doi: 10.1016/j.proenv.2012.01.090

[25] National Satellite Meteorological Center, "FY-2 satellite products and data format", Meteorological Press, Beijing, 1-10pp, 2008.

[26] J. Yang., C.H. Dong, N.M. Lu., Z.H.D. Yang, J.M. Shi, P. Zhang., Y.J. Liu., B. Cai., "FY-3A: the new generation polar-orbiting meteorological satellite of China", Acta

© 2013 ACADEMY PUBLISHER

Meteorologica Sinica, Chinese Meteorological Society, vol. 67, no. 4, pp.501-509, 2009. doi: 10.1175/2009BAMS2798.1

[27] B.H. Tang, Y.Y. Bi, Z.L. Li, J. Xia, "Generalized split-window algorithm for estimate of land surface temperature from Chinese geostationary FengYun meteorological satellite (FY-2C) data", Sensors, Molecular Diversity Preservati, vol. 8, no. 2, pp.933–951, 2008. doi: 10.3390/s8020933

[28] J. Andersen, I. Sandholt, K.H. Jensen, J.C. Refsgaard, Gupta H., "Perspectives in using a remotely sensed dryness index in distributed hydrological models at the river-basin scale", Hydrological Processes, Wiley, vol.16, no. 15, pp.2973–2987, 2002. doi: 10.1002/hyp.1080

© 2013 ACADEMY PUBLISHER